Plasma Models for Real-Time Control of Advanced Tokamak Scenarios

D. Moreau 1), D. Mazon 1), M. L. Walker 2), J. R. Ferron 2), S. M. Flanagan 2), P. Gohil 2), R. J. Groebner 2), R. J. La Haye 2), E. Schuster 3), Y. Ou 3), C. Xu 3), Y. Takase 4), Y. Sakamoto 5), S. Ide 5), T. Suzuki 5), and ITPA-IOS group members and experts

1) CEA, IRFM, 13108 Saint-Paul-lez-Durance, France
2) General Atomics, San Diego, CA 92186, USA
3) Lehigh University, Bethlehem, PA 18015, USA
4) The University of Tokyo, 277-8561, Kashiwa, Japan
5) Japan Atomic Energy Agency, Naka, Ibaraki 311-0193, Japan

E-mail contact of main author: didier.moreau@cea.fr

Abstract. An integrated plasma profile control strategy, ARTAEMIS, is being developed for extrapolating present-day advanced tokamak (AT) scenarios to steady state operation. The approach is based on semi-empirical (grey-box) modeling. It was initially explored on JET, for current profile control only (D. Moreau, *et al*., Nucl. Fus. 48 (2008) 106001). The present paper deals with the generalization of this strategy to *simultaneous magnetic and kinetic control*. The determination of the *device-specific, control-oriented models* that are needed to compute optimal controller matrices *for a given operation scenario* is discussed. The methodology is generic and can be applied to any device, with different sets of heating and current drive actuators, controlled variables and profiles. The system identification algorithms take advantage of the large ratio between the magnetic and thermal diffusion time scales and have been recently applied, in their full version, to both JT-60U and DIII-D data. On JT-60U, an existing series of high-bootstrap-current (~70%), 0.9 MA non-inductive AT discharges was used. The actuators consisted of four groups of neutral beam injectors aimed at perpendicular injection (on-axis and off-axis), and co-current tangential injection (also on-axis and off-axis). On DIII-D, dedicated open-loop modulation experiments were carried out. The reference plasma state was that of a 0.9 MA AT scenario which had been optimized to combine non-inductive current fractions near unity with $3.5 < \beta_N < 3.9$, bootstrap current fractions larger than 65%, and $H_{98(y,2)}=1.5$. DIII-D was operated in the loop voltage (V_{ext}) control mode (as opposed to current control) to avoid feedback in the response data from the primary circuit. Actuators other than V_{ext} were co-current, counter-current and balanced neutral beam injection, and electron cyclotron current drive. Power and loop voltage modulations resulted in dynamic variations of the plasma current between 0.7 and 1.2 MA. It is concluded that the response of several essential plasma parameter profiles to the specific actuators of a given device can be satisfactorily identified from a small set of experiments. This provides, for control purposes, a *readily available* alternative to first-principle plasma modeling.

1. Introduction

The design of an economically attractive steady state fusion reactor relies on the development of the so-called advanced tokamak (AT) operation scenarios in which an optimization of some plasma parameter profiles results in a large improvement in fusion performance, at reduced plasma current [1-3]. A high-gain fusion burn could then be achieved while a major fraction of the toroidal current is self-generated by the neoclassical bootstrap effect. However, in present-day experiments, the high performance phase is often limited in duration by transport and MHD phenomena. Real-time control of the magneto-thermal plasma state is therefore needed for the extrapolation of the scenarios to steady state operation.

In a tokamak, the multiple magnetic and kinetic profiles which define the plasma state (poloidal magnetic flux, safety factor, plasma density, velocity, pressure, etc …) are known to be strongly coupled. Although non-linear, the linkage between these profiles can be seen as an advantage because the effective number of controlled parameters and profiles can be reduced to a minimal set of essential ones. Once the response of these profiles to variations of the actuators around a given equilibrium has been identified, an integrated controller can be designed to regulate the global plasma state through a minimization algorithm, rather than

each plasma parameter or profile accurately and separately. For any chosen set of target profiles, the *closest self-consistent plasma state achievable with the available actuators* will then be reached. The main features of a set of identification and control algorithms based on this strategy, hereafter refered to as the ARTAEMIS approach, were described in reference [4] together with some preliminary experiments performed on JET. A general state-space model structure was derived from a simplified set of transport equations which are projected on a set of appropriate radial basis functions. The model order is then further reduced by using the theory of singularly perturbed systems in which the small parameter, ε, represents the typical ratio of the thermal and resistive diffusion timescales. Starting from a set of appropriate data, the ARTAEMIS algorithms generate a slow and a fast dynamic model, as well as the near-optimal two-time-scale controller corresponding to these coupled models [5].

This paper focuses on the identification of *control-oriented magneto-kinetic plasma models* from the analysis of experimental data. A physics-based empirical approach is followed ("grey-box" modeling), motivated by the fact that present understanding of plasma transport phenomena is not sufficient yet to make real-time first principle predictions of the detailed dynamic response of the plasma profiles. The next section describes the choice of the relevant state variables, and the structure of the reduced state-space models. Then, in section 3, the method is applied to existing JT-60U data, for the coupled response of the safety factor and toroidal rotation profiles to four neutral beam actuators. In section 4, dedicated experiments performed on DIII-D are described, and the results of the ARTAEMIS model identification for the coupled dynamics of the poloidal magnetic flux and toroidal rotation are reported.

2. Two-time-scale state-space structure of the dynamic plasma models

When the usual set of plasma transport equations are averaged over magnetic flux surfaces they yield a one-dimensional model in which all physical variables depend only on a radial variable, x, and on time. The system is linearized around an equilibrium state which is refered to as the *reference state*, and *which needs not be known explicitly*. A state space model of minimal complexity is then found [4], within assumptions that have been made to keep the system order within reasonable limits and its experimental identification tractable. The state variables appear naturally to be the variations of the internal poloidal magnetic flux, Ψ, and a set of fluid/kinetic variables such as the plasma density, n, toroidal velocity, V_Φ, and temperature, T (ideally $[T_i, T_e]$), with respect to their reference values. One can then introduce some unknown linear differential operators, $\mathcal{L}_{\alpha,\beta}\{x\}$, and row vectors, $L_{\alpha,\beta}(x)$, depending upon the variable x but independent of time, such that the system under consideration reads :

$$\frac{\partial \Psi(x,t)}{\partial t} = \mathcal{L}_{\Psi,\Psi}\{x\} \circ \Psi(x,t) + \mathcal{L}_{\Psi,K}\{x\} \circ \begin{bmatrix} n(x,t) \\ V_\Phi(x,t) \\ T(x,t) \end{bmatrix} + L_{\Psi,P}(x) \cdot P(t) + V_{ext}(t) \qquad (1a)$$

$$\varepsilon \frac{\partial}{\partial t} \begin{bmatrix} n(x,t) \\ V_\Phi(x,t) \\ T(x,t) \end{bmatrix} = \mathcal{L}_{K,\Psi}\{x\} \circ \Psi(x,t) + \mathcal{L}_{K,K}\{x\} \circ \begin{bmatrix} n(x,t) \\ V_\Phi(x,t) \\ T(x,t) \end{bmatrix} + L_{K,P}(x) \cdot P(t) \qquad (1b)$$

with inputs $P(t) = [P_1(t), P_2(t), P_3(t), \text{etc} \ldots]$, the heating, fueling and current drive inputs, e.g. powers from neutral beam injection (NBI), ion cyclotron resonance heating (ICRH), electron cyclotron or lower hybrid current drive (ECCD, LHCD), gas flow, etc ..., and V_{ext}, the plasma

surface loop voltage. After projection onto radial basis functions (e.g. cubic splines), a lumped-parameter version of the state space model is then derived, which reads :

$$\dot{\Psi}(t) = A_{1,1}\cdot \Psi(t) + A_{1,2}\cdot \begin{bmatrix} n(t) \\ V_{\Phi}(t) \\ T(t) \end{bmatrix} + B_1\cdot P(t) + B_{\Psi,V}\cdot V_{ext}(t) \tag{2a}$$

$$\varepsilon \begin{bmatrix} \dot{n}(t) \\ \dot{V}_{\Phi}(t) \\ \dot{T}(t) \end{bmatrix} = A_{2,1}\cdot \Psi(t) + A_{2,2}\cdot \begin{bmatrix} n(t) \\ V_{\Phi}(t) \\ T(t) \end{bmatrix} + B_2\cdot P(t) \tag{2b}$$

where parameter profiles are now represented by vectors, A_{hk} , B_h (with h = 1, 2 and k = 1, 2) are unknown matrices and $B_{\Psi,V}$ is a known matrix. It is clear from the structure of the original system that the magnetic variable, Ψ(t), has only a slow evolution. Following Ref. 5, we shall therefore seek two models of reduced orders, a slow model:

$$\dot{\Psi}(t) = A_S\cdot \Psi(t) + B_S\cdot \begin{bmatrix} P_S(t) \\ V_{ext,S}(t) \end{bmatrix} \qquad \text{with} \qquad \begin{bmatrix} n_S(t) \\ V_{\Phi,S}(t) \\ T_S(t) \end{bmatrix} = C_S\cdot \Psi(t) + D_S\cdot P_S(t) \tag{3}$$

and a fast model:

$$\begin{bmatrix} \dot{n}_F(t) \\ \dot{V}_{\Phi,F}(t) \\ \dot{T}_F(t) \end{bmatrix} = A_F\cdot \begin{bmatrix} n_F(t) \\ V_{\Phi,F}(t) \\ T_F(t) \end{bmatrix} + B_F\cdot P_F(t) \tag{4}$$

where any input or kinetic variable, X, is to be split into a slow and a fast component, X_S and X_F, respectively, according to $X = X_S + X_F$. The slow linkage between the magnetic equilibrium and the kinetic profiles is represented, in its linearized form, by the C_S matrix.

Now, although the poloidal magnetic flux appears as a natural state variable, one may find more practical to perform magnetic control through the inverse safety factor profile, ι(*x*), a non-dimensional parameter that is defined by $\iota(x) = 1/q(x) = d\Psi(x)/d\Phi(x)$ where Φ(*x*) is the toroidal magnetic flux. At constant toroidal field and plasma shape, and when the radial variable, *x*, is defined as $(\Phi/\Phi_{max})^{1/2}$ where Φ_{max} is the toroidal flux within the last closed flux surface, Φ(*x*) depends weakly on the power inputs in comparison with Ψ(*x*). Thus, for control purposes, an alternative state-space model can be sought where the linearized variations of ι(*x*) around a given equilibrium are assumed to map onto those of Ψ(*x*), so that ι(*x*) can be substituted to Ψ(*x*) in equations (3), and assumed to be the magnetic state variable. This substitution was made for magnetic profile control experiments on JET [4] and will be illustrated in section 3, while Ψ(*x*) will be retained as the magnetic state variable in section 4.

3. System identification from existing JT-60U data

The first extended version of the ARTAEMIS identification algorithm that allows a two-time-scale *magneto-kinetic model* to be identified has been developed using existing JT-60U data typical of steady state AT operation. A series of high-bootstrap-current discharges [6] were

analysed (pulses #45862, and #45903-45914) and an iterative identification procedure was set up. It allows the matrices A_S, B_S, C_S, D_S, A_F and B_F to be chosen in such a way that the model structure described above (Eqs. 3-4) fits the data at best, while satisfying some mathematical and physical constraints that reduce the dimensionality of the unknown parameter space.

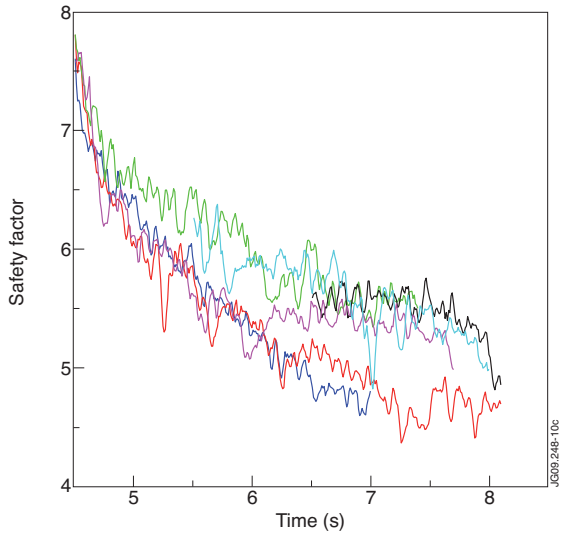

FIG. 1a. Time evolution of the safety factor at x =0.6 in JT-60U pulses #45903-04-06-07-09-14.

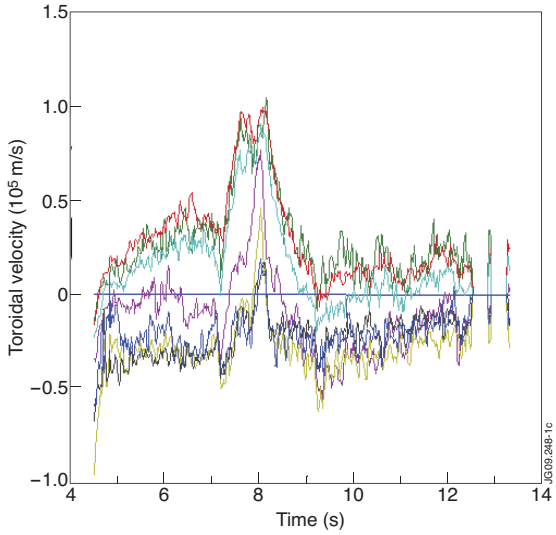

FIG. 1b. Time evolution of the toroidal velocity (10^5 m/s) at x = 0.2, 0.3, 0.4, 0.5, 0.6, 0.7 and 0.8 in JT-60U pulse #45903.

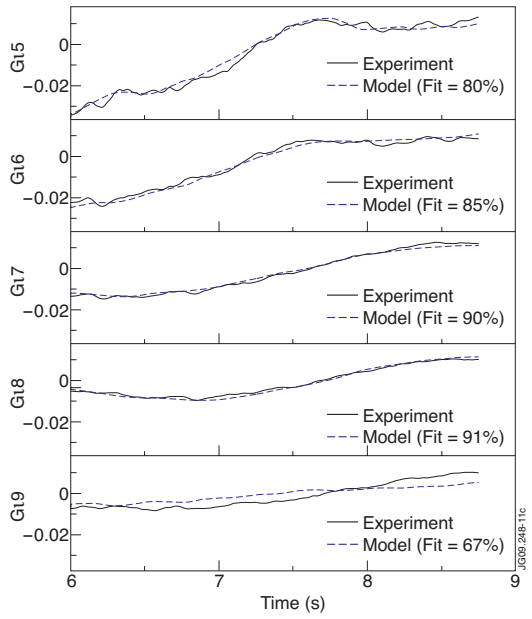

FIG. 2. Comparison between the measured (black) and model-simulated (blue) ι =1/q data versus time, at x = 0.5, 0.6, 0.7, 0.8 and 0.9 (JT-60U pulse #45862).

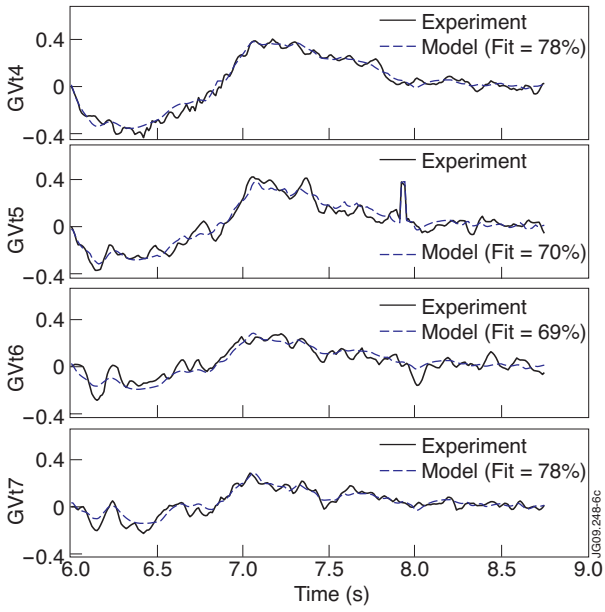

FIG. 3. Comparison between the measured (black) and model-simulated (blue) V_ϕ data (10^5 m/s) versus time, at x = 0.4, 0.5, 0.6 and 0.7 (fast model, JT-60U pulse #45862).

The reference plasma state was characterized by a magnetic field of 3.7 T, a fully non-inductive plasma current of 0.9 MA, and a central plasma density of 3×10^{19} m^{-3}. The selected actuators consisted of four groups of neutral beam injectors corresponding to : *(i)* on-axis perpendicular injection, *(ii)* off-axis perpendicular injection, *(iii)* on-axis co-current tangential injection, *(iv)* off-axis co-current tangential injection. The selected output profiles were the

inverse safety factor, $\iota(x)$, toroidal rotation velocity, $V_\phi(x)$, and ion temperature, $T_i(x)$. Typical data used for system identification can be seen on Fig.1. Fig. 1a shows the time evolution of the safety factor at x=0.6 in various pulses in which the actuator inputs varied, and Fig. 1b shows the evolution of the toroidal velocity at x=0.2 , 0.3, … 0.8 in pulse #45903. The large change in plasma rotation between t=7s and 8s is mainly due to the replacement of 2 MW of tangential injection by 2 MW of perpendicular injection.

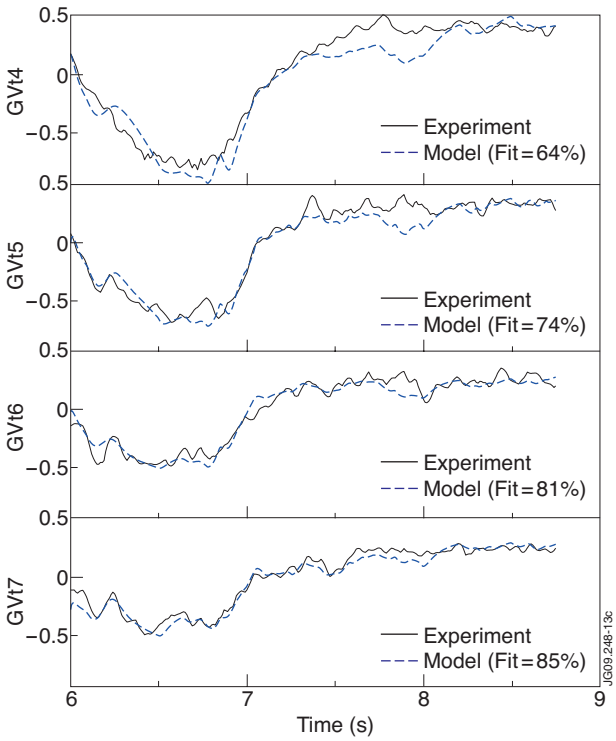

FIG. 4. Comparison between the measured (black) and model-simulated (blue) V_ϕ data (10^5 m/s) at x = 0.4, 0.5, 0.6 and 0.7 (full model, JT-60U pulse #45862).

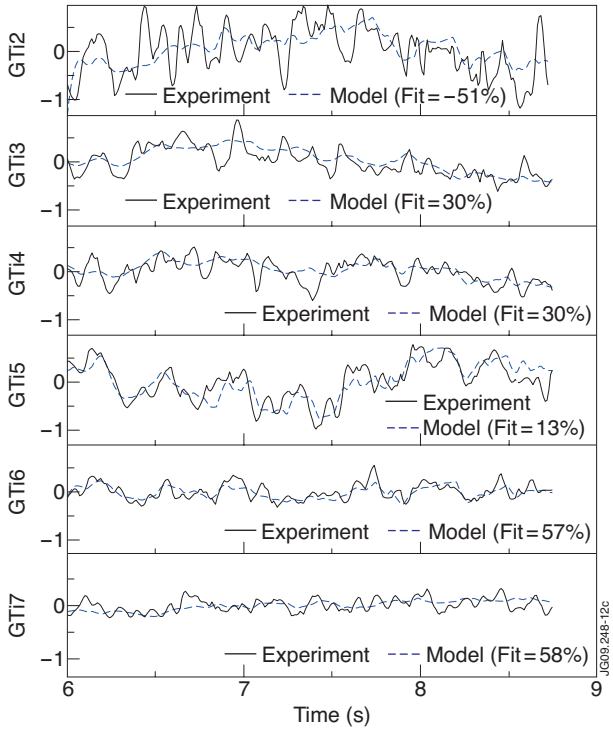

FIG. 5. Comparison between the measured (black) and model-simulated (blue) T_i data (keV) at x = 0.2, 0.3, 0.4, 0.5, 0.6 and 0.7 (full model, JT-60U pulse #45862).

The system identification was performed through a number of iterations in which the data is projected onto subspaces of increasing dimensions, along a general methodology described in Ref. 4. The splitting between the slow and the fast components of the data was made here by filtering the data with a cutoff frequency of 1.25 Hz. Fig. 2-5 illustrate typical comparisons between the measured data and the model simulation at the radii for which data was available. Examples of the slow model response (Eq. 3) for $\iota(x) = 1/q(x)$ and of the fast model response (Eq. 4) for $V_\phi(x)$ are shown on Fig. 2 and 3, respectively (the fast component of $\iota(x)$ that can be seen on Fig. 1a was attributed to noise, and disregarded). The full model response (Eq. 3-4) for $V_\phi(x)$ and $T_i(x)$ is shown on Fig. 4 and 5, respectively, for the same discharge.

4. System identification experiments on DIII-D

In order to assess the generic character of the semi-empirical ARTAEMIS approach for control-oriented plasma modeling and controller design, a set of dedicated experiments has been performed on DIII-D. The reference plasma state was that of a 1.8 Tesla β_N-controlled AT scenario, at a central plasma density, $n_{e0} \approx 3.5 \times 10^{19}$ m^{-3} and plasma current, I_p = 0.9 MA. The scenario had been developed to combine non-inductive current fractions near unity with normalized pressure $3.5<\beta_N<3.9$, bootstrap current fractions larger than 65%, and a

normalized confinement factor, $H_{98(y,2)} \approx 1.5$ [7]. Available beamlines and gyrotrons were grouped to form, together with V_{ext} (Eq. 1), five independent H&CD actuators: *(i)* co-current NBI power, P_{CO}, *(ii)* counter-current NBI power, P_{CNT}, *(iii)* balanced NBI power, P_{BAL}, *(iv)* total ECCD power from all gyrotrons in a fixed off-axis current drive configuration, P_{EC}, and *(v)* V_{ext}. Actuator modulations were applied from t = 2.5 s, i.e. after 1 s of a 0.9 MA current flat top. At this time, in all discharges, the V_{ext} control mode was enabled and the I_p and β_N controls were disabled in order to avoid feedback in the response from the actuators while using V_{ext} as an actuator[1]. 23 such discharges were obtained, with I_p modulations in the range 0.7-1.2 MA. The undesired but measured variations of two additional inputs to the system were treated as disturbances: The gas injection flow rate, P_{GAS}, that was used in a density control loop, and the power, P_{CER}, from a beamline that was used for diagnostic purposes. Fig. 6a-b display typical modulations of the system inputs and of I_p, line-averaged density and β_N.

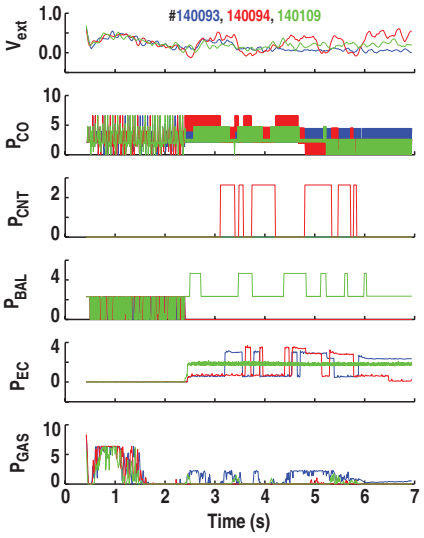

FIG. 6a. Time evolution of V_{ext}, P_{CO}, P_{CNT}, P_{BAL}, P_{EC}, and P_{GAS} in DIII-D shots #140093, 140094, and 140109.

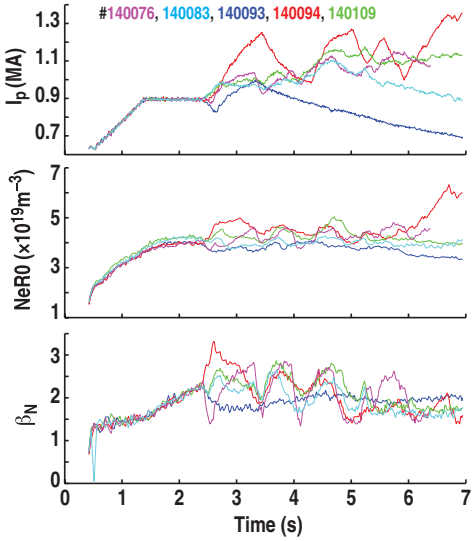

FIG. 6b. Time evolution of I_p, line-averaged density and β_N in DIII-D shots #140076, 140083, 140093, 140094, and 140109.

System identification for the internal poloidal flux, $\Psi(x)$, was first carried out, and Fig. 7 illustrates the typical fits obtained. It must be noted that shots #140075 (Fig. 7, left) and #140094 (Fig. 7, right) were not used in the identification process, and that, for all discharges, the model fits the data satisfactorily from t = 1 s, i.e. also during the current ramp-up phase, despite the fact that the data used for model identification was taken after 1 s of flat-top (t > 2.5 s). Another feature of interest is that 8 discharges in which an n=1 neo-classical tearing mode was present were disregarded for identification, but they also produced satisfactory fits for $\Psi(x)$ from this relatively robust magnetic model (see Fig. 7, left). Then, given the matrices A_S and B_S, a two-time-scale model for the coupled evolution of $\Psi(x)$ and $V_\phi(x)$ was sought. A cutoff frequency of 1 Hz was found to be adequate for separating the slow and fast components of the input and rotation data. Fig. 8 illustrates typical fits obtained for $V_\phi(x)$.

The steady state gain matrix and the eigenmodes of the system constitute the essential elements of the identified linear state space model. Fig. 9 shows the steady state increment of the poloidal flux and plasma rotation profiles upon unit increment of the various inputs in the

[1] Controlled steady state operation could thus be readily obtained by letting the weight of V_{ext} vanish with respect to other actuators in the controller gain matrices, when sufficiently close to the required plasma state.

model. The smallest eigenvalues of the slow and fast models correspond to a characteristic resistive time of 5.4 s and a momentum confinement time of 0.16 s, respectively.

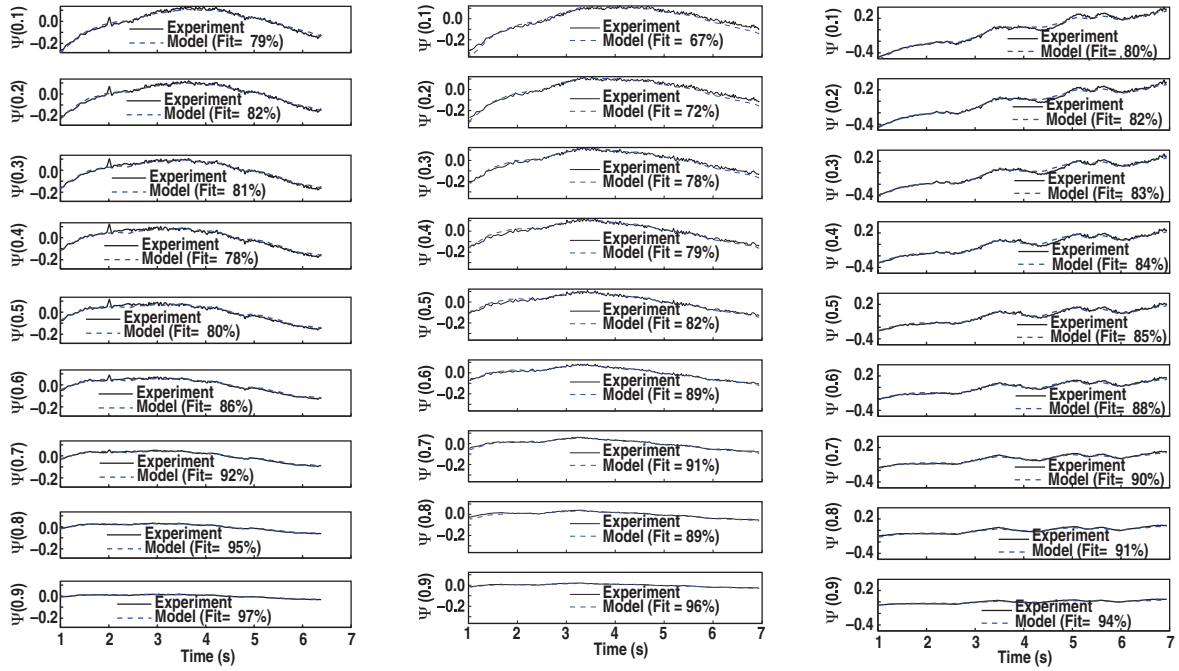

FIG. 7. Comparison between the measured (black) and model-simulated (blue) Ψ data (Wb) at x = 0.1 , 0.2, ... 0.9 for DIII-D shots #140075 (left), 140090 (center) and 140094 (right).

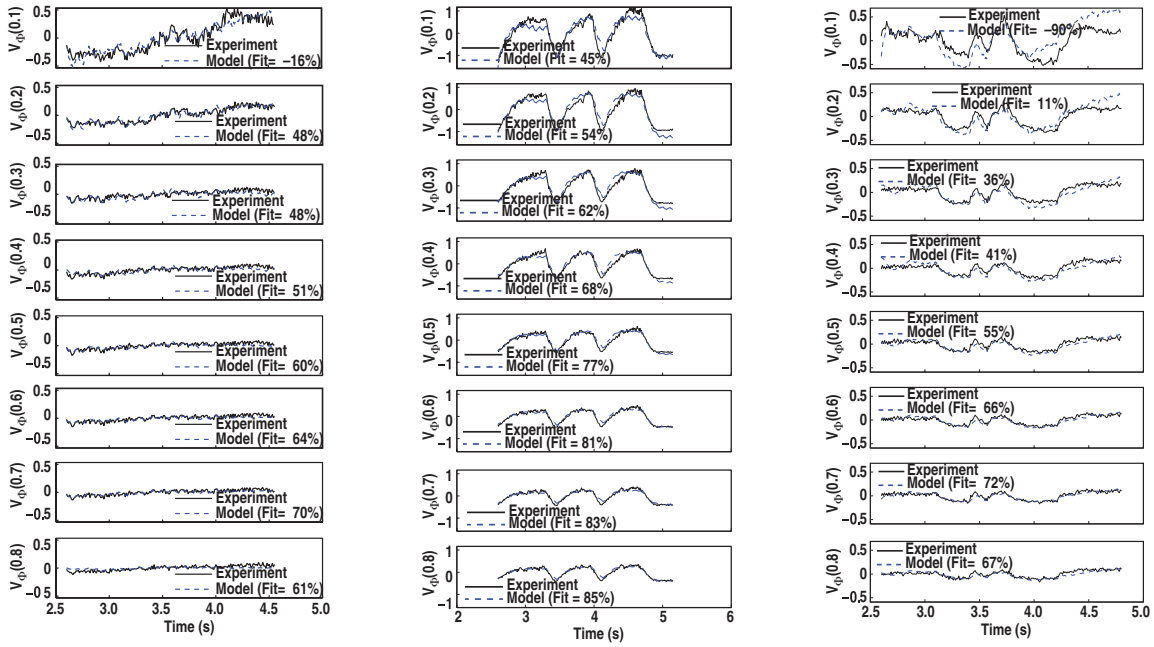

FIG. 8. Comparison between the measured (black) and model-simulated (blue) V_ϕ data at x = 0.1 , 0.2, ... 0.8 for DIII-D shots #140074 (left), 140076 (center) and 140106 (right).

5. Conclusion

The semi-empirical method described here yields models that reproduce satisfactorily the coupled dynamics of the parameter profiles around a given scenario, and therefore provides,

for control purposes, a *readily available* alternative to first-principle plasma modeling. It can be applied to different tokamaks, with different set of actuators and sensors and is therefore generic. The experimental identification of such *control-oriented* models will open the way to the development of real-time profile control for advanced plasma scenarios, a requirement for steady state tokamak operation. New experimental investigations will be necessary, on a variety of existing devices, to validate such models and the controllers based on them. They may provide a lead for developing advanced plasma control in ITER.

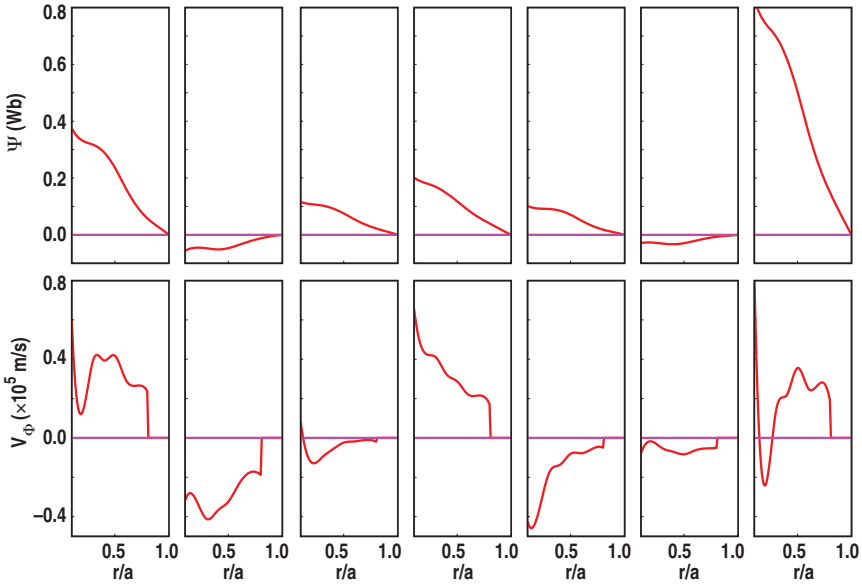

FIG. 9. Representation of the model steady state gain matrix. Each column represents the variation of the poloidal flux (top) and toroidal rotation (bottom) profiles corresponding to unit positive step variation of a given input. Columns #1-7 correspond to P_{CO} (MW), P_{CNT} (MW), P_{BAL} (MW), P_{CER} (MW), P_{EC} (MW), P_{GAS} (10 Torr.l/s) and V_{ext} (0.1 Volt), respectively.

Acknowledgements

This work, supported by the European Communities under the contract of Association between EURATOM and CEA, was carried out within the framework of the European Fusion Development Agreement and in part by the US Department of Energy under DE-FC02-04ER54698 and DE-FG02-92ER54141. The views and opinions expressed herein do not necessarily reflect those of the European Commission. The first author is very grateful to the Takase-Ejiri Laboratory (University of Tokyo), the JT-60U Team and the DIII-D Team, for their support and hospitality.

References

[1] ROMANELLI, F., KAMENDJE, R., on behalf of JET-EFDA Contributors, Nucl. Fusion **49** (2009) 104006.
[2] OYAMA, N., and the JT-60 Team, Nucl. Fusion **49** (2009) 104007.
[3] STRAIT, E. J., for the DIII-D Team, Nucl. Fusion **49** (2009) 104008.
[4] MOREAU, D., et al., Nucl. Fusion **48** (2008) 106001.
[5] KOKOTOVITCH, P.V., KHALIL, H.K., O'REILLY, J., "Singular Perturbation Methods in Control: Analysis and Design", Academic Press, London (1986).
[6] SAKAMOTO, Y., et al., Nucl. Fusion **49** (2009) 095017.
[7] HOLCOMB, C. T., et al., Phys. of Plasmas **16** (2009) 056116.